

## Synthesis and characterization of maleated rosin-modified fluorosilicone resin and its fluorosilicone rubber

Tao Xu,<sup>1,3</sup> He Liu,<sup>1</sup> Jie Song,<sup>2</sup> Shi-bin Shang,<sup>1</sup> Zhanqian Song,<sup>1</sup> Kaifei Zou,<sup>3</sup> Chong Yang<sup>3</sup>

<sup>1</sup>Institute of Chemical Industry of Forestry Products, Chinese Academy of Forestry, Key Laboratory of Biomass Energy and Material, National Engineering Laboratory for Biomass Chemical Utilization, Key and Open Laboratory on Forest Chemical Engineering, SFA, Nanjing, 210042, Jiangsu, People's Republic of China

<sup>2</sup>Department of Chemistry and Biochemistry, University of Michigan-Flint, Flint, Michigan 48502

<sup>3</sup>Shenzhen Guanheng New Materials Technology Co., Ltd, Shenzhen 518109, Guangdong, China

Correspondence to: S. Shang (E-mail: shangsb@hotmail.com) and Z. Song (E-mail: lhssxly@hotmail.com)

**ABSTRACT:** Imide-containing vinyl fluorosilicone resin (MR-VFS) was synthesized from maleated rosin (MR). And then, with MR-VFS as a new polar cross-linking agent in a heat curable fluorosilicone rubber composition, a series of maleated rosin-modified fluorosilicone rubbers (MR-FSR) were obtained. The effects of MR-VFS on the mechanical properties, oil resistance, thermal stability, and low-temperature performance were studied in detail. It was found that MR-VFS could increase the tearing strength and high-temperature thermal stability of fluorosilicone rubber. When the MR-VFS weight content reached to 2 wt %, the tearing strength of MR-FSR increased by 20.1% compared with that of common fluorosilicone rubber. However, MR-FSR showed a similar low-temperature resistance and a little worse oil resistance. The morphological study showed that incorporation of maleated rosin could intensify the microphase separation of fluorosilicone rubber. © 2015 Wiley Periodicals, Inc. *J. Appl. Polym. Sci.* **2015**, *132*, 41888.

**KEYWORDS:** copolymers; elastomers; grafting; morphologies; properties and characterization

Received 11 August 2014; accepted 14 December 2014

DOI: 10.1002/app.41888

### INTRODUCTION

Fluorosilicone combines the structures of fluorocarbon and polysiloxane. It has the unique properties of heat resistance, low-temperature flexibility, and fuel resistance.<sup>1–10</sup> It offers the best low-temperature properties of any oil-resistant rubber and is primarily used in fuel delivery systems of automobiles, aeronautics and astronautics.<sup>15</sup> However, similar to all silicone rubbers, it has the drawback of relatively low mechanical strength because of the weak intermolecular forces among polysiloxane chains. To improve the mechanical strength, especially the tearing strength, vinyl-containing silicone resin has been used as cross-linking agent.<sup>11</sup>

Polyimide is an important class of high-performance materials and has outstanding comprehensive properties such as excellent thermo-oxidative stability, mechanical strength, electrical properties, and high solvent resistance.<sup>12</sup> And all these properties are more due to the strong rigidity and polarity of imide heterocycle. Theoretically, grafting imide heterocycle onto flexible fluorosilicone chain would be a promising approach to increase the mechanical strength.<sup>13</sup> Poly(methyltrifluoropropylsiloxane-

block-imide) copolymers have been prepared by the thermal imidization of carboxylic dianhydride and aminopropyl-terminated fluorosilicone prepolymer.<sup>14</sup> However, effects of imide on the mechanical strength of fluorosilicone rubber have rarely been reported.

The decrease in petroleum has led to research and development activities worldwide for the use of alternative resource material for polymers.<sup>15–17</sup> Maleated rosin (MR) is the Diels-Alder adduct of natural rosin and maleic anhydride and mainly contains maleopimaric acid (MPA) and others resin acid.<sup>17</sup> So maleated rosin is a very promising thermal imidization reagent.

In this study, imide-modified vinyl fluorosilicone resin (MR-VFS) was synthesized by the imidization of maleated rosin with amino group in the side chain of fluorosilicone. After then, with MR-VFS as a new polar cross-linking agent in a heat curable fluorosilicone rubber composition, a series of maleated rosin-modified fluorosilicone rubbers (MR-FSR) were obtained. Effects of MR-VFS on the mechanical properties, oil resistance, low-temperature performance, and thermal stability were studied in detail. It was found that maleated rosin could increase

Additional Supporting Information may be found in the online version of this article.

© 2015 Wiley Periodicals, Inc.

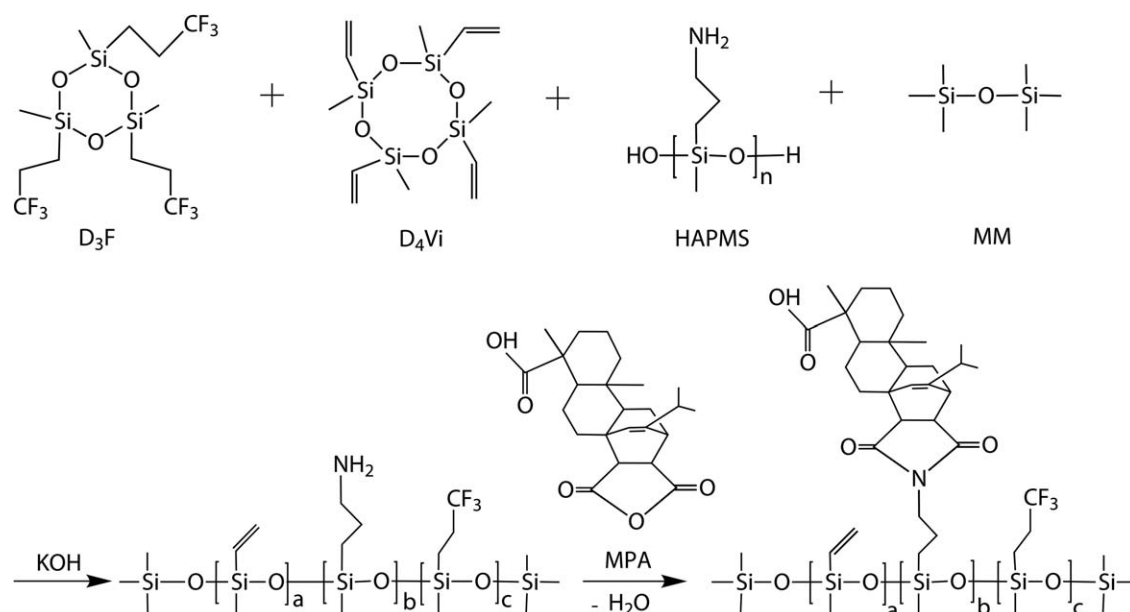


Figure 1. Preparation scheme of maleated rosin-modified vinyl fluorosilicone resin (MR-VFS).

the mechanical properties and thermal stability of fluorosilicone rubber. The morphology was also investigated by scanning electron microscope (SEM) and energy-dispersive X-ray spectroscopy (EDX).

## EXPERIMENTAL

### Materials

D<sub>3</sub>F (1,3,5-tris((3,3,3-trifluoropropyl)methyl)cyclotrisiloxane, purity  $\geq 99.5\%$ ) was supplied by Shenzhen Guanheng New Materials Technology. HAPMS was obtained from the hydrolyzation of 3-aminopropyl(diethoxy)methylsilane and then dehydrated under vacuum at 100°C for 8 h, and its chemical structure could be found in Figure 1. Fluorosilicone gum (poly(methyltrifluoropropylsiloxane-co-methylvinylsiloxane), the weight percent of vinyl group was 0.16% and the viscosity-average molecular weight was  $1.1 \times 10^6$ ) was obtained according to literature.<sup>18</sup> Fluorosilicone oil (a silanol end-stoped poly(methyltrifluoropropylsiloxane) with a viscosity of 104 MPa s) was obtained according to literature.<sup>19</sup> Fumed silica HDK®N20 was purchased from Wacker. MR (maleated rosin, 115) was purchased from Wuzhou Sun Shine Forestry and Chemicals. All the other chemicals were of analytical reagent grade and purchased from J&K Scientific.

### Characterization

<sup>1</sup>H NMR and <sup>13</sup>C NMR analyses were conducted with a Bruker DRX-500 nuclear magnetic resonance spectrometer with tetramethylsilane as the internal standard. Mechanical properties were measured in accordance with ASTM D412, D624, D792–2008, and D2240. Differential scanning calorimetry (DSC) measurements were performed on a Perkin-Elmer Diamond DSC instrument at a heating rate of 10°C min<sup>-1</sup>. The thermogravimetric analysis (TGA) was performed on a TG209F1 thermogravimetric analyser at a heating rate of 10°C min<sup>-1</sup> in a nitrogen flow (2 mL min<sup>-1</sup>). The morphology was also investigated by scanning electron microscope (SEM; JSM-7600F,

JEOL) and energy-dispersive X-ray spectroscopy (EDX; X-ACT) on the new cut surfaces of FSR, which were sputter coated with platinum.

Average cross-link densities ( $\gamma_e$ ) of the samples were calculated from data obtained in the mechanical analysis according to the following equation<sup>20</sup>:

$$\gamma_e = \frac{\sigma}{\rho RT(\alpha - \alpha^{-2})} \quad (1)$$

where  $\sigma$  is the tensile strength,  $\rho$  is the density, and of rubber,  $R$  is 8.31 J/(mol·K)<sup>-1</sup>,  $T$  is room temperature, and  $\alpha$  is breaking elongation.

According to ASTM D471, oil resistance of FSR was measured by the percent change of mechanical properties before and after immersed in ASTM reference fuel C at 25°C for 72 h. The mechanical strength ( $P$ ), including tensile strength, breaking elongation, and tearing strength, was measured, and their percent changes ( $\Delta P\%$ ) were calculated according to the following eq. (2):

$$\Delta P\% = \frac{P_i - P_o}{P_i} \times 100\% \quad (2)$$

where  $P_i$  is the initial mechanical strength before immersion,  $P_o$  is the mechanical strength after immersion.

The percent change in volume ( $\Delta V\%$ ) was calculated by the following eq. (3):

$$\Delta V\% = \frac{(M_3 - M_4) - (M_1 - M_2)}{(M_1 - M_2)} \times 100\% \quad (3)$$

where  $M_1$  is the initial mass of specimen in air,  $M_2$  is the initial mass of specimen in water,  $M_3$  is the mass of specimen in air after immersion, and  $M_4$  is the mass of specimen in water after immersion.

### Synthesis of Vinyl Fluorosilicone Resin

Maleated rosin-modified vinyl fluorosilicone resin (MR-VFS) was prepared by a one-pot synthesis process without using any

**Table I.** Weight Parts and Weight Percent of Vinyl-Containing Fluorosilicone Resin (VFS) in the Formulae of FSR

Sample	MR-VFS		C-VFS	
	Parts	wt %	Parts	wt %
P-FSR	0	0	0	0
C-FSR1	0	0	1.5	1.0
C-FSR2	0	0	3.0	2.0
C-FSR3	0	0	4.5	3.0
C-FSR4	0	0	6.0	4.0
MR-FSR1	1.5	1.0	0	0
MR-FSR2	3.0	2.0	0	0
MR-FSR3	4.5	3.0	0	0
MR-FSR4	6.0	4.0	0	0

solvent. Firstly, 10 g of D<sub>3</sub>F, 12.5 g of hexamethyldisiloxane, 28.1 g of 1,3,5,7-tetravinyl-1,3,5,7-tetramethylcyclotetrasiloxane, 20.8 g of HAPMS and 0.1 wt % of potassium hydroxide were dehydrated at 50°C and polymerized at 100°C for 12 h. After that, 69.5 g of MR was added and slowly heated to 150°C in about 4 h. Finally, the product was slowly vacuumed to remove the volatile at about 180°C. The above preparation scheme of MR-VFS was presented in Figure 1.

As a contrast, a common vinyl fluorosilicone resin (C-VFS) was prepared in accordance with the aforementioned process, except that the mass of D<sub>3</sub>F was adjusted to 100.3 g with HAPMS and MR absent.

### Preparation of Fluorosilicone Rubber

In order to study the effect of MR on the fluorosilicone rubber, the MR-VFS and C-VFS obtained previously were added into a common heat curable fluorosilicone rubber composition,<sup>1,2,21</sup> which would be adjusted for a better processability in this study. Firstly, 100 weight parts of fluorosilicone gum, 7.2 weight parts of fluorosilicone oil, and needed parts of VFS were blended in a vacuum kneader at room temperature. Then, HDK®N20 was mixed step by step. MR or fumed silica would significantly increase the viscosity of fluorosilicone rubber composition and finally increase the difficulty of rubber processing. In order to obtain a good processability, the loading of HDK®N20 was chosen as 36.4 weight parts according to our previous study and the reported literature.<sup>21</sup> After that, the mixing temperature was increased to 150°C and kept at a pressure of 30 mmHg for 6 h. After being cooled to room temperature, based on 100 weight parts of the obtained above mixtures, 0.5 weight parts of DBPH were mixed uniformly using a two roll. The ultimate fluorosilicone rubber samples (FSR) were compression molded at 170°C under a pressure of 10 MPa and postcured at 200°C for 2 h. All FSR samples, including MR-FSR, C-FSR, and P-FSR, were prepared in accordance with the aforementioned process except for the content of VFS. The needed parts and weight percent of VFS in the formula of FSR were presented in Table I.

## RESULTS AND DISCUSSION

### Characterization of MR-Modified Vinyl Fluorosilicone Resin

The structures of C-VFS and MR-VFS were determined by <sup>1</sup>H NMR and <sup>13</sup>C NMR. Their <sup>1</sup>H NMR spectra were shown in

Figure 2. And the typical peaks of C-VFS at 0–0.3 ppm (Si-CH<sub>3</sub>), 0.7–0.8 ppm (Si-CH<sub>2</sub>), 2.0–2.3 ppm (–CH<sub>2</sub>CF<sub>3</sub>) and 5.6–6.2 ppm (Si-CH=CH<sub>2</sub>) could be observed in Figure 2(a).<sup>4</sup> In contrast to the spectrum of C-VFS, there were different peaks occurred in the spectrum of MR-VFS. The peak at 5.4 ppm should be attributed to CH=C in maleated rosin; the signal in the range of 3.1–3.4 ppm should be the protons (O=CCHCHC=O) on the imide heterocycle; the peak at 3.0 ppm should be attributed to the N-CH<sub>2</sub>, which were connected with the imide heterocycle; the other peaks in the ranges of 4.5–5.3 ppm and 0.3–2.9 ppm should be attributed to maleated rosin and SiCH<sub>2</sub>CH<sub>2</sub>.<sup>22</sup>

The <sup>13</sup>C NMR spectra of C-VFS and MR-VFS were shown in Figure 3. And the typical carbon peaks of C-VFS at –1.5 ppm (SiCH<sub>3</sub>), 8.5 ppm (SiCH<sub>2</sub>), 26–27 ppm (–CH<sub>2</sub>CF<sub>3</sub>), 132–136 ppm (Si-CH=CH<sub>2</sub>) could be observed in Figure 3(a), while the carbon peaks of –CF<sub>3</sub> (125 ppm) were not obvious.<sup>23</sup> The peak at 76 ppm was produced by the solvent CDCl<sub>3</sub>. In Figure 2(b), the typical carbon peaks of MR appeared at 184 ppm (COOH), 175–179 ppm (carbons in the imide heterocycle), 145 ppm (CH=C) and 124 ppm (CH=C).<sup>22</sup> The other carbon peaks of maleated rosin were widely distributed in the range of 10–150 ppm.

The NMR spectra of MR-VFS were more complex than C-VFS. However, the characteristic peaks of maleated rosin-modified fluorosilicone resin (MR-VFS) could be observed in the <sup>1</sup>H NMR and <sup>13</sup>C NMR spectra. These signals, especially the peaks of CH=C and O=C–N–C=O, strongly proved that MR-based fused ring (MRBFR) had been successfully grafted onto the side chain of fluorosilicone polymer. The grafting reactions were mainly realized by the amidization and imidization of carbonyl group (O=C) in MR and primary amino group (H<sub>2</sub>N–) in the side chain of fluorosilicone polymer (Figure 1).<sup>12</sup>

With the significant difference in molecular structure, MR could not dissolve in the fluorosilicone polymer to form a homogeneous solution. So any unreacted MR would precipitate from reaction product. However, in this study, the obtained reaction product of MR and fluorosilicone polymer was homogeneous, which strongly demonstrated the formation of chemical bonding between MR and fluorosilicone polymer and completion of the grafting reaction.

MR-VFS was a complex mixture and maybe useful in fluorosilicone rubber modification. With the equivalent molecular weight, C-VFS was clear liquid at room temperature, while MR-VFS was brown powder. This convincingly demonstrated that MRBFR could increase the cohesion energy (*E*<sub>coh</sub>) of fluorosilicone polymer. To improve the tearing strength of silicone rubber, the vinyl-containing silicone resin had always been used as a cross-linking agent in heat-curable silicone rubber.<sup>11</sup> With MR-VFS as a substitute for conventional cross-linking agent, maleated rosin-modified fluorosilicone rubber (MP-FSR) would be prepared and characterized in the following text.

### Mechanical Properties

The mechanical properties of FSR were listed in Table II, and effects of VFS on the tearing strength of FSR were presented in

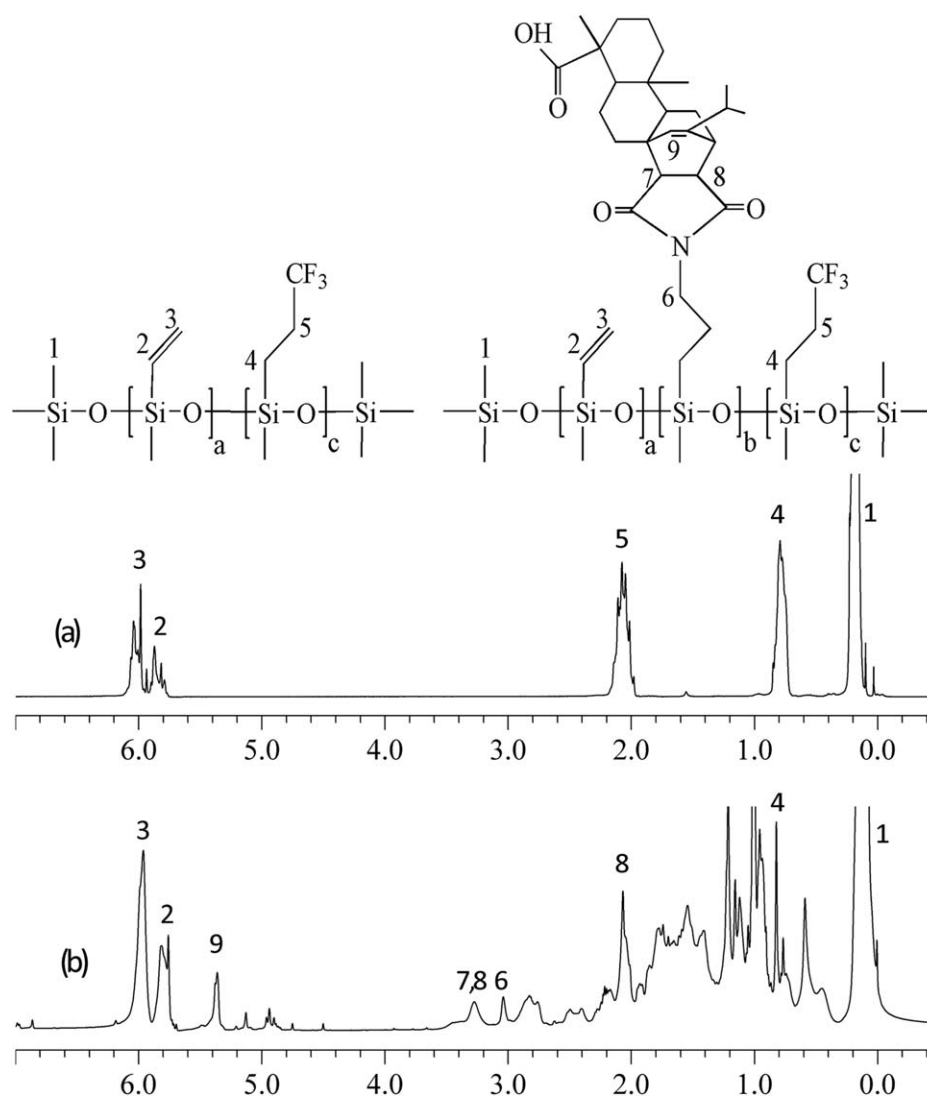


Figure 2.  $^1\text{H}$  NMR spectra of C-VFS (a) and MR-VFS (b) in  $\text{CDCl}_3$ .

Figure 4. Although the tensile strength and hardness of MR-FSR were not improved by the incorporation of polar MRBFR, the tearing strength and breaking elongation were effectively improved. These mechanical improvements should be due to the increase in  $E_{\text{coh}}$ ,<sup>13,24</sup> which was resulted by the incorporation of polar MRBFR.

As was shown in Figure 4, the tearing strength of MR-FSR increased initially with the increasing content of MR-VFS and decreased rapidly after the content of MR-VFS exceeded 2 wt %. When the VFS content was less than 2 wt %, MR-FSR behaved better tearing resistance than C-FSR and P-FSR. When the VFS content was at 2 wt %, the tearing strength of MR-FSR increased by 20.1% (compared with C-FSR) and 9.1% (compared with P-FSR). It could be concluded that MR-VFS (or MRBFR) could significantly improve the tearing strength of fluorosilicone rubber, even though a little amount of MR-VFS (or MRBFR) was added in the fluorosilicone rubber. However, when the VFS content exceeded 2 wt %, the tearing strength of MR-FSR decreased rapidly, and the hard-

ness showed the similar trend. It was known that both tearing strength and hardness have a close relation with cross-link density in rubber.<sup>11,13,20</sup> So it was necessary to study the cross-link density of MR-FSR.

Average cross-link densities ( $\gamma_e$ ) of FSR were calculated according to eq. (1) and listed in Table II. It could be observed that hardness of C-FSR increased as C-VFS content and  $\gamma_e$  went up, that is to say, the  $\gamma_e$  of C-FSR had a positive correlation with hardness.<sup>24</sup> This indicated that C-VFS could increase the cross-link density of fluorosilicone rubber and further result in the increase in hardness. It could be predicted that the tearing strength and hardness of MR-FSR would decrease with the decreasing  $\gamma_e$  of MR-FSR on the overall trend in a much wider range of MR-VFS content (e.g., 0–10 wt %). However, the above regulation of C-FSR seemed to be not applicable to MR-FSR in this paper when MR-VFS content was less than 4.0 wt %. The  $\gamma_e$  of MR-FSR decreased with the increase of MR-VFS content, which showed a different change trend from the hardness and tearing strength.

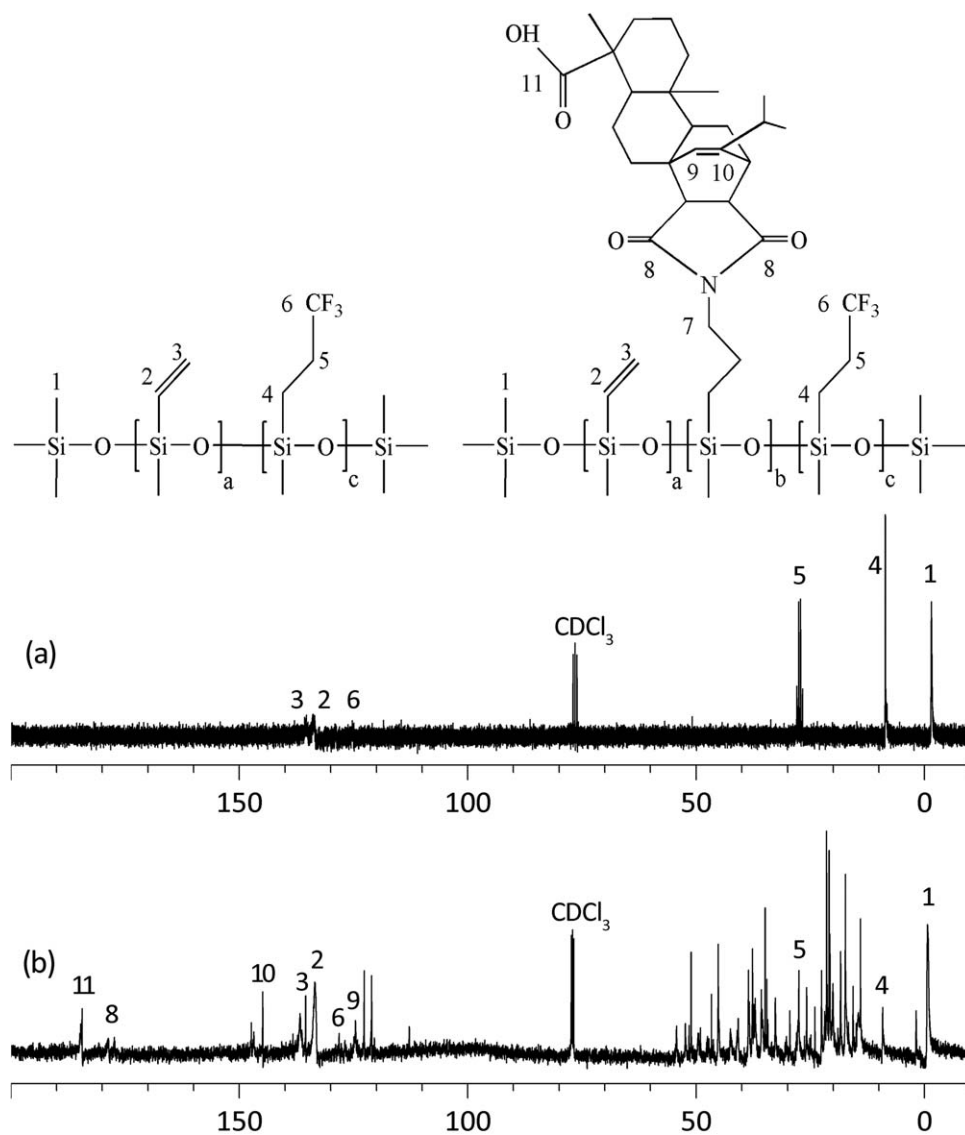
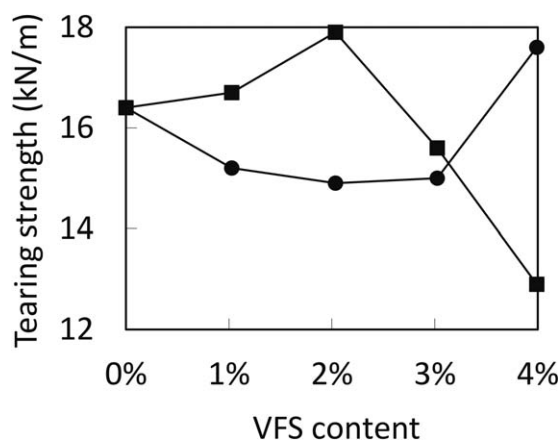


Figure 3.  $^{13}\text{C}$  NMR spectra of C-VFS (a) and MR-VFS (b) in  $\text{CDCl}_3$ .

Table II. Mechanical Properties and Average Cross-Link Density ( $\gamma_e$ ) of FSR Before Immersed in Oil

Sample	Density ( $\text{g cm}^{-3}$ )	Tensile strength (MPa)	Breaking elongation (%)	Hardness (Shore A)	Cross-linking density ( $\gamma_e$ ) ( $\text{mol m}^{-3}$ )
P-FSR	1.459	9.2	202	62	12.8
C-FSR1	1.457	8.7	197	63	12.4
C-FSR2	1.450	8.2	177	65	13.1
C-FSR3	1.446	8.1	172	66	13.4
C-FSR4	1.449	8.1	168	68	13.7
MR-FSR1	1.455	7.1	211	62	9.49
MR-FSR2	1.452	6.0	256	65	6.63
MR-FSR3	1.448	3.6	272	64	3.75
MR-FSR4	1.444	2.1	184	63	3.24



**Figure 4.** Tearing strength of fluorosilicone rubber with varying contents of VFS resin (■- MR-FSR; ○- C-FSR).

It seemed that both hardness and tearing strength of MR-FSR tended to have closer relation with the sum of  $\gamma_e$  and  $E_{coh}$ , because  $E_{coh}$  could also resist the tearing force and increase the hardness.<sup>24</sup> With the increase in MR-VFS content, MR-FSR'  $E_{coh}$  would increase, while its  $\gamma_e$  showed an opposite trend. In theory, there was a possibility that the maximum value of their sum would occur at 2 wt %. That is to say, the sum of  $\gamma_e$  and  $E_{coh}$  increased initially with the increasing content of MR-VFS and decreased after the content of MR-VFS exceeded 2 wt %.

#### Oil Resistance

The mechanical strength of FSR was measured after immersed in ASTM reference fuel C at 25°C for 72 h. As was shown in Figure 5, the percent change in the tearing strength of MR-FSR was larger than that of C-FSR but was still smaller than that of P-FSR. So MR-FSR behaved better oil resistance than P-FSR in respect of tearing strength. The percent changes in tensile strength, breaking elongation and volume were all listed in Table III. It could be found that there was no obvious difference among them. In sum, it could be concluded that MR-FSR behaved a little worse oil resistance than C-FSR, but better than P-FSR.

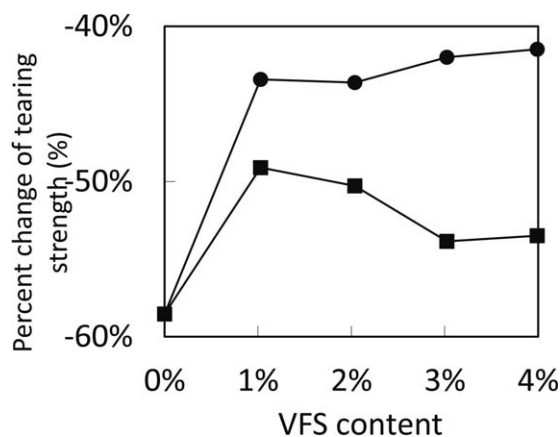


**Figure 5.** Percent change in the tearing strength of fluorosilicone rubber after immersed in oil with varying contents of VFS resin (■- MR-FSR; ○- C-FSR).

**Table III.** Percent Change in Mechanical Properties of Fluorosilicone Rubber After Immersed in Oil

Sample	Tensile strength %	Breaking elongation %	Volume %
P-FSR	-45.0	-33.6	16.7
C-FSR1	-44.1	-33.9	16.3
C-FSR2	-43.1	-32.1	16.1
C-FSR3	-46.8	-35.9	15.8
C-FSR4	-47.4	-38.0	16.1
MR-FSR1	-47.0	-35.1	16.7
MR-FSR2	-45.7	-28.4	17.1
MR-FSR3	-51.3	-31.2	18.0
MR-FSR4	-54.9	-38.8	18.0

#### Thermal Stability

Thermal stability of FSR was investigated by TGA in nitrogen atmosphere, and the results could be found in Supporting Information Figures S1 and S2. P-FSR, C-FSR2, and MR-FSR2 were taken as examples and their corresponding results were presented in Figure 6. The  $T_5$  (the temperature corresponding to the mass loss = 5%) of P-FSR, C-FSR2, and MR-FSR2 were, respectively, 457.7, 452.8, and 437.5°C. Although MR-FSR2 showed the worst thermal stability before 450°C, the mass loss of MR-FSR2 did not exceed 7%. This decline of thermal stability for MR-FSR2 should be due mainly to the decrease of cross-link density in fluorosilicone rubber.

The obvious weight losses from all samples began around 450°C and were all complete by 600°C. The values of  $T_{max}$  (the temperature corresponding to the weight-loss rate-maximum in the DTG curve) were, respectively, 507.7°C (P-FSR), 526.5°C (C-FSR1), 523.6°C (C-FSR2), 522.8°C (C-FSR3), 522.1°C (C-FSR4), 539.2°C (MR-FSR1), 527.3°C (MR-FSR2), 526.7°C (MR-FSR3), and 517.0°C (MR-FSR4). Compared with C-FSR and P-FSR, MR-FSR showed better thermal stability at high temperature, which should be due to the presence of imide heterocycle.<sup>12,14</sup>

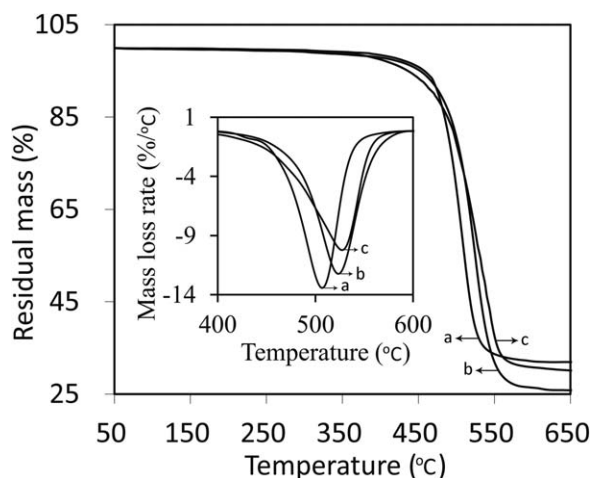


**Figure 6.** TG and DTG curves of P-FSR (a), C-FSR2 (b), and MR-FSR2 (c).

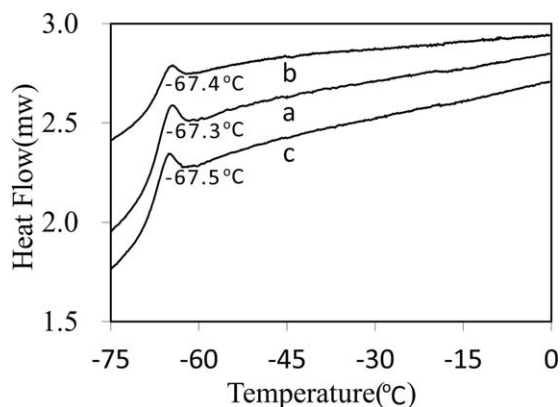


**Figure 7.** DSC curves of P-FSR (a), C-FSR2 (b), and MR-FSR2 (c).

The final residual mass ratio of P-FSR, C-FSR2, and MR-FSR2 at 800°C was, respectively, 32.2%, 25.8%, and 29.8%. Although their VFS contents were equal, MR-FSR2 presented a higher residual mass ratio than C-FSR2. Thus, it could be predicted that the incorporation of MR in fluorosilicone rubber was helpful to the formation of residue such as SiO<sub>2</sub> or silicon-oxy-carbide under thermal degradation.<sup>7</sup>

In sum, it could be concluded that incorporation of maleated rosin (or MRBFR) could improve the high temperature thermal stability of fluorosilicone rubber.

#### Low-Temperature Resistance

The low-temperature performance was investigated by DSC in the temperature range of -75°C to 0°C, and the results could be found in Supporting Information Figures S3 and S4. All of the DSC curves showed a similar change trend. P-FSR, C-FSR2, and MR-FSR2 were taken as examples and presented in Figure 7. Their glass transition temperature ( $T_g$ ) were, respectively, -67.3°C (P-FSR), -67.6°C (C-FSR1), -67.4°C (C-FSR2), -67.5°C (C-FSR3), -67.6°C (C-FSR4), -67.9°C (MR-FSR1), -67.5°C (MR-FSR2), -68.0°C (MR-FSR3), and -68.1°C (MR-FSR4). So it could be concluded that MR-FSR performed similar low-temperature resistance with ordinary fluorosilicone rubber.

#### Morphology

The above special properties of MR-FSR should be correlated with its microscopic structure. Since MR-VFS contains both imide heterocycle and phenanthrene ring (i.e., MRBFR), it should have more stronger polarity and rigidity than fluorosilicone polymer. In theory, this difference in the polarity and rigidity would lead to the phase separation between MRBFR and fluorosilicone polymer.<sup>25</sup> Actually, the similar microphase separation between imide segment and silicone segment had been observed in poly(methyltrifluoropropylsiloxane-*b*-imide) copolymer by SEM.<sup>14</sup> Besides, the aggregation of hydrogenated rosin in pressure-sensitive adhesives was also reported.<sup>26</sup>

In this study, morphologies of P-FSR, C-FSR, and MR-FSR were investigated by means of SEM. P-FSR, C-FSR2, and MR-FSR2 were taken as examples to study the effect of MR-VFS on the morphology of FSR, and their corresponding SEM images were presented in Figure 8. The white and spherical domains should be fumed silica, while the left domain was heterogeneous and

should be the polymer phase, in which microphase separation could be observed. It could be found that the degree of the micro-phase separation was in the following order: P-FSR < C-FSR < MR-FSR.

According to the previous study,<sup>11</sup> the network of P-FSR should be formed by “Dispersive Cross-linking” [Figure 9(a)], when C-VFS was used as the cross-linking agent, “Concentrative Cross-linking” [Figure 9(b)] should be formed in C-FSR, which made its microphase separation stronger than that of P-FSR. Based on this, when MR-VFS was used as the cross-linking agent in MR-FSR, driven by the polarity and rigidity of MRBFR, “Concentrative Cross-linking” seemed to aggregate further and ultimately form the gray and scattered domain in Figure 9(c).

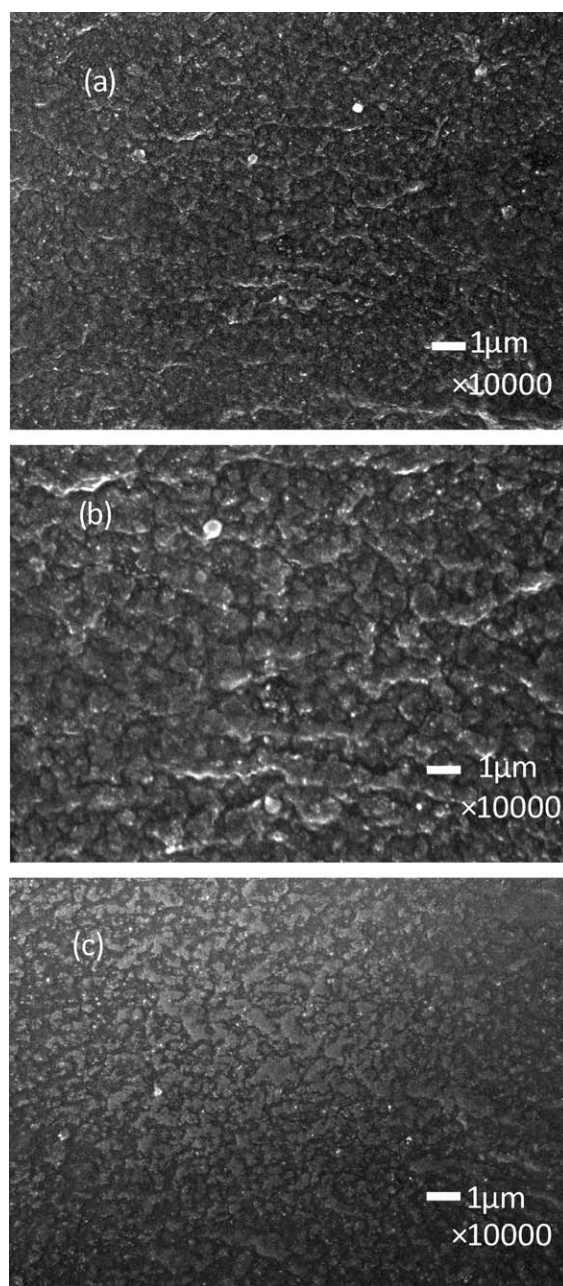


**Figure 8.** SEM images of (a) P-FSR, (b) C-FSR2, and (c) MR-FSR2.

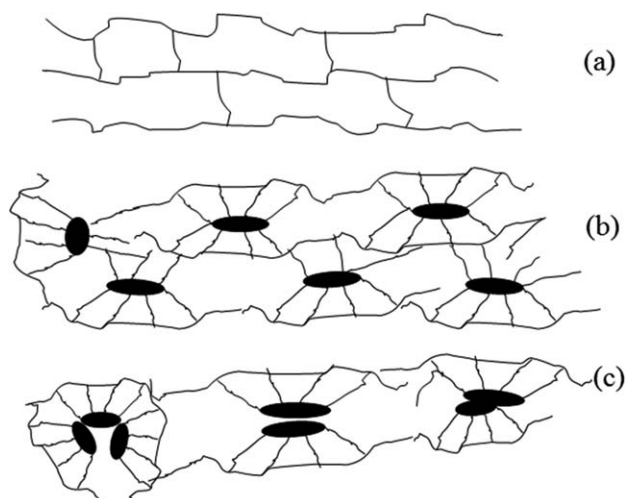


**Figure 9.** Cross-linking network of (a) pure fluorosilicone rubber P-FSR<sup>11</sup>, (b) C-VFS modified fluorosilicone rubber (C-FSR2)<sup>11</sup>, and (c) MR-VFS modified fluorosilicone rubber (MR-FSR2).

Consequently, the polymer phase in MR-FSR could be classified into hard phase and soft phase. The gray and scattered phase in the SEM image of MR-FSR should be the hard phase, which was formed by the aggregation of MRBFR; the black and continuous phase should be the soft phase, which was formed by the aggregation of poly(methyltrifluoropropylsiloxane). The SEM images of MR-FSR1, MR-FSR3, and MR-FSR4 could be found in Supporting Information Figure S5.

In order to verify our assumption, EDX was used to identify the elemental composition of both the hard phase and soft phase, and the obtained figures were presented in Figure 10. As was shown in Figure 10(a), EDX was carried out in two representative locations: location 1 represented the composition of hard phase, while location 2 represented that of soft phase. Their corresponding elemental analysis curves were presented in Figure 10(b,c). It could be observed that the weight concentration of the element C in location 1 was higher than that in

**Table IV.** Elemental Composition of the Polymer Phase in MR-FSR

Atomic percent (%)	C	O	F	Si
Location 1	74.4	13.4	6.9	5.3
Location 2	30.2	34.4	16.5	18.9

location 2. The atomic percent of carbon was calculated and present in Table IV. The atomic percent of carbon in location 1 was almost 1.5 times larger than that in location 2. Considering that the carbon content of MRBFR was higher than that of poly(methyltrifluoropropylsiloxane), the aggregation of MRBFR in hard phase could be demonstrated.

Aggregation of MRBFR intensified the microphase separation in the polymer phase of MR-FSR, widened the distribution of the hard phase size, and led to a more random molecular arrangement, which resulted in the decrease in density of MR-FSR compared with P-FSR and C-FSR (Table II). The cohesion energy  $E_{\text{coh}}$  of hard phase was also improved significantly, which result in the increase of tearing strength and breaking elongation.

## CONCLUSIONS

Maleated rosin had been successfully grafted on the side chain of vinyl-containing fluorosilicone resin. This maleated rosin-modified vinyl-containing fluorosilicone resin (MR-VFS) contained imide heterocycle and had more polarity than common vinyl-containing fluorosilicone resin (C-VFS). With MR-VFS as a new polar cross-linking agent in a heat curable fluorosilicone rubber composition, a series of maleated rosin-modified fluorosilicone rubbers (MR-FSR) were obtained and characterized in detail. It was found that maleated rosin could increase the tearing strength effectively. When the MR-VFS weight content reached to 2 wt %, the tearing strength of MR-FSR increased by 20.1% compared with that of common fluorosilicone rubber (C-FSR). Maleated rosin also increased high-temperature thermal stability in some extent. The  $T_{\text{max}}$  of MR-FSR2 increased by 3.7°C than that of C-FSR2, and 19.6°C than that of P-FSR.

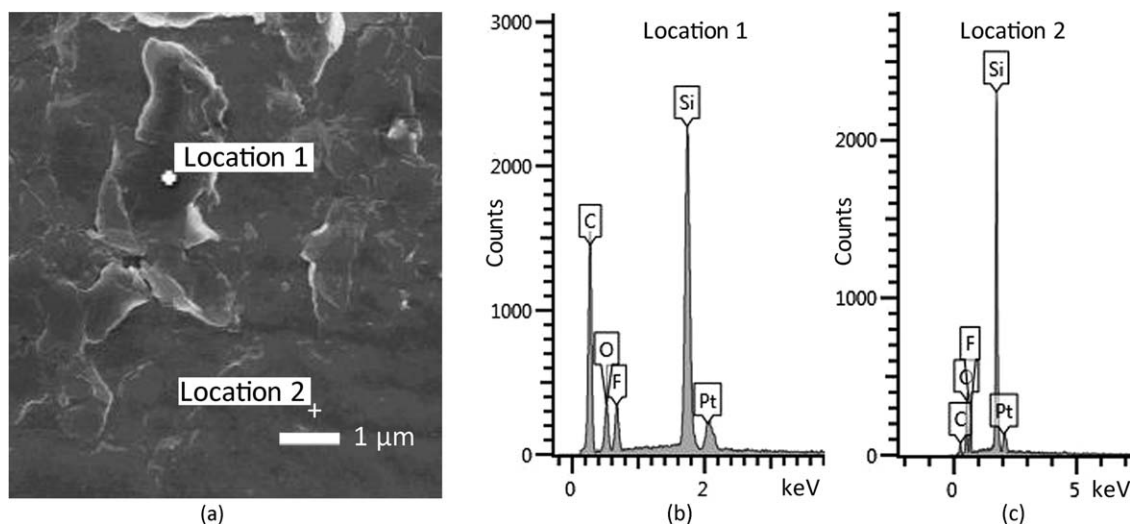


**Figure 10.** EDX (a) and elemental analysis (b,c) for MR-FSR2 (the sample point was marked with the white cross).



However, MR-FSR showed a similar low-temperature resistance and a little worse oil resistance. The morphological study showed that incorporation of maleated rosin could intensify the microphase separation of fluorosilicone rubber.

#### ACKNOWLEDGMENTS

This study was financially supported by the National Natural Science Foundation of China (Grant No. 31200446).

#### REFERENCES

1. Liu, Y.; Zhou, C.; Feng, S. *Mater. Lett.* **2012**, *78*, 110.
2. Liu, Y.; Liu, H.; Zhang, R.; Zhou, C.; Feng, S. *Polym. Eng. Sci.* **2013**, *53*, 52.
3. Lina, C.; Chien, C.; Tan, J.; Chao, Y. J.; Van Zee, J. W. *J. Power Sources* **2011**, *196*, 1955.
4. Li, B.; Chen, S.; Zhang, J. *Polym. Chem.* **2012**, *9*, 2366.
5. Kählig, H.; Zöllner, P.; Mayer-Helm, B. X. *Polym. Degrad. Stab.* **2009**, *94*, 1254.
6. Gao, Y.; Jiang, W.; Guan, Y.; Yang, P.; Zheng, A. *Polym. Eng. Sci.* **2010**, *50*, 2440.
7. Li, B.; Chen, S.; Zhang, J. *J. Appl. Polym. Sci.* **2014**, *131*, 39708.
8. Furukawa, Y.; Shin-Ya, S.; Miyake, H.; Kishino, H.; Yamada, M.; Kato, H.; Sato, M. *J. Appl. Polym. Sci.* **2001**, *82*, 3333.
9. Yi, L.; Huang, C.; Zhou, W. *J. Polym. Sci. Part A: Polym. Chem.* **2012**, *50*, 1728.
10. Yi, L.; Zhan, X.; Chen, F.; Du, F.; Huang, L. *J. Polym. Sci. Part A: Polym. Chem.* **2005**, *43*, 4431.
11. Zhao, S.; Feng, S. *J. Appl. Polym. Sci.* **2002**, *83*, 3123.
12. Sheng, S.; Zhang, W.; Lu, C.; Wan, J.; Liu, X.; Song, C. *J. Appl. Polym. Sci.* **2014**, *126*, 297.
13. He, P. S. *Structure and Properties of Polymers*; Alpha Science International Ltd: Oxford, **2012**.
14. Kang, D. W.; Kim, Y. M. *J. Appl. Polym. Sci.* **2002**, *85*, 2867.
15. Deng, L.; Shen, M.; Yu, J.; Wu, K.; Ha, C. *Ind. Eng. Chem. Res.* **2012**, *51*, 8178.
16. Wilbon, P. A.; Zheng, Y.; Yao, K.; Tang, C. *Macromolecules* **2010**, *43*, 8747.
17. Xu, X.; Shang, S.; Song, Z.; Cui, S.; Wang, H.; Wang, D. *Bioresources* **2011**, *6*, 2460.
18. Kobayashi, H.; Nishiumi, W. *Macromol. Chem. Phys.* **1993**, *194*, 1404.
19. Cypryk, M.; Delczyk, B.; Juhari, A. *J. Polym. Sci. Part A: Polym. Chem.* **2009**, *47*, 1204.
20. Han, Y.; Zhang, J.; Shi, L.; Qi, S.; Chen, J.; Jin, R. *Polym. Degrad. Stab.* **2008**, *93*, 245.
21. Takita, K. U. S. Pat. 6,369,155 **2002**.
22. Wang, J. F.; Chen, Y. P.; Yao, K.; Wilbon, P. A.; Zhang, W.; Ren, L.; Zhou, J.; Nagarkatti, M.; Wang, C.; Chu, F.; He, X.; Decho, A. W.; Tang, C. *Chem. Commun.* **2011**, *48*, 917.
23. Fujino, M.; Hisaki, T.; Fujiki, M.; Matsumoto, N. *Macromolecules* **1992**, *25*, 1080.
24. Zhang, D. R.; Xing, Z. X. *Advanced Rubber Formulation Design*; Chemical Industry Press: Beijing, **2011**.
25. Mark, J. E.; Erman, B. *Rubberlike Elasticity: A Molecular Primer*; Wiley: New York, **2007**.
26. Jeusette, M.; Peeterbroeck, S.; Simal, F.; Cossement, D.; Roose, P.; Leclère, Ph.; Dubois, Ph.; Hecq, M.; Lazzaroni, R. *Eur. Polym. J.* **2008**, *44*, 3931.